JACS
JOURNAL OF THE AMERICAN CHEMICAL SOCIETY
pubs.acs.org/JACS
Article

Optical and EPR Detection of a Triplet Ground State Phenyl Nitrenium Ion

Yunfan Qiu, Lili Du, Sarah D. Cady, David Lee Phillips,* and Arthur H. Winter*

Cite This: J. Am. Chem. Soc. 2024, 146, 10679−10686
Read Online
ACCESS | Metrics & More | Article Recommendations | Supporting Information

ABSTRACT: Nitrenium ions are important reactive intermediates participating in the synthetic chemistry and biological processes. Little is known about triplet phenyl nitrenium ions regarding their reactivity, lifetimes, spectroscopic features, and electronic configurations, and no ground state triplet nitrenium ion has been directly detected. In this work, *m*-pyrrolidinyl-phenyl hydrazine hydrochloride (**1**) is synthesized as the photoprecursor to photochemically generate the corresponding *m*-pyrrolidinyl-phenyl nitrenium ion (**2**), which is computed to adopt a π, π^* triplet ground state. A combination of femtosecond (fs) and nanosecond (ns) transient absorption (TA) spectroscopy, cryogenic continuous-wave electronic paramagnetic resonance (CW-EPR) spectroscopy, computational analysis, and photoproduct studies was performed to elucidate the photolysis pathway of **1** and offers the first direct experimental detection of a ground state triplet phenyl nitrenium ion. Upon photoexcitation, **1** forms S1, where bond heterolysis occurs and the NH_3 leaving group is extruded in 1.8 ps, generating a vibrationally hot, spin-conserving closed-shell singlet phenyl nitrenium ion (^{1}**2**) that undergoes vibrational cooling in 19 ps. Subsequent intersystem crossing takes place in 0.5 ns, yielding the ground state triplet phenyl nitrenium ion (^{3}**2**), with a lifetime of 0.8 μs. Unlike electrophilic singlet phenyl nitrenium ions, which react rapidly with nucleophiles, this triplet phenyl nitrenium reacts through sequential H atom abstractions, resulting in the eventual formation of the reduced *m*-pyrrolidinyl-aniline as the predominant stable photoproduct. Supporting the triplet ground state, continuous irradiation of **1** in a glassy matrix at 80 K in an EPR spectrometer forms a paramagnetic triplet species, consistent with a triplet nitrenium ion.

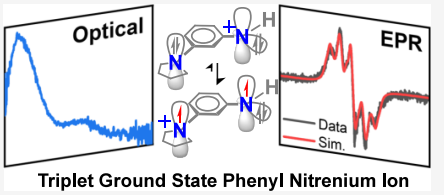

INTRODUCTION

Nitrenium ions are reactive intermediates with the general formula of RNR'$^+$, which are isoelectronic with carbenes but have a positive charge on a hypovalent nitrogen atom.[1,2] Biochemically, nitrenium ions are formed by metabolic oxidation of aromatic amines[3] found in charred meats and dyes,[4] etc. They can also be generated chemically or photochemically as reactive synthetic intermediates. In particular, aryl nitrenium ions, denoted as Ar-NR$^+$, have been extensively studied driven by their presence in synthetic chemistry[5] and biological processes as suspected carcinogens capable of causing DNA damage and modification.[6−10]

Generally, most aryl nitrenium ions (Ar-NH$^+$) have closed-shell singlet ground states with large singlet−triplet gaps resulting from a strong break in the degeneracy of the *p* orbitals on the formal nitrenium center, whose vacant *p* orbital receives the electron density contribution from the filled π orbital of the aromatic ring. For example, the parent phenyl nitrenium ion is predicted to be a singlet ground state species with a singlet−triplet energy, ΔE_{ST}, of −20 kcal/mol to an *n*, π^* triplet state (a negative value for ΔE_{ST} indicates a singlet ground state).[11]

In contrast to the many studies of singlet aryl nitrenium ions, there remains a dearth of knowledge regarding the reactivity, lifetimes, spectroscopic features, and electronic configurations of triplet phenyl nitrenium ions, because the triplet state is usually not the energetically preferred ground state. Experimental exploration of an *N-tert*-butyl aryl nitrenium ion, conducted by Falvey et al., inferred the intermediacy of a triplet species based on indirect product studies using external triplet photosensitizers and H atom donors.[12,13] Only recently was the first triplet nitrenium ion observed, the *n*, π * triplet *p*-iodo-phenyl nitrenium ion, as depicted in Figure 1. This system harnessed the heavy atom effect and rapid intersystem crossing (ISC) by employing an iodine atom to generate an *n*, π^* triplet nitrenium ion in its excited triplet state. In that case, the excited triplet undergoes ISC into the ground singlet state, preventing a study of its reactivity but providing a first glimpse at an elusive triplet phenyl nitrenium ion.[14]

Nevertheless, to date, a direct optical or EPR detection of a triplet ground state phenyl nitrenium ion remains unattained despite several computational studies that have predicted the existence of triplet ground state aryl nitrenium ions.[15−18] A computational study investigating the impact of *meta* substitution on the ΔE_{ST} (singlet−triplet energy gap) of phenyl nitrenium ions revealed that substituting the *meta*

Received: January 11, 2024
Revised: March 13, 2024
Accepted: March 14, 2024
Published: April 5, 2024

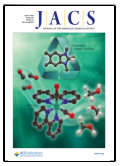

https://doi.org/10.1021/jacs.4c00511
J. Am. Chem. Soc. 2024, 146, 10679−10686

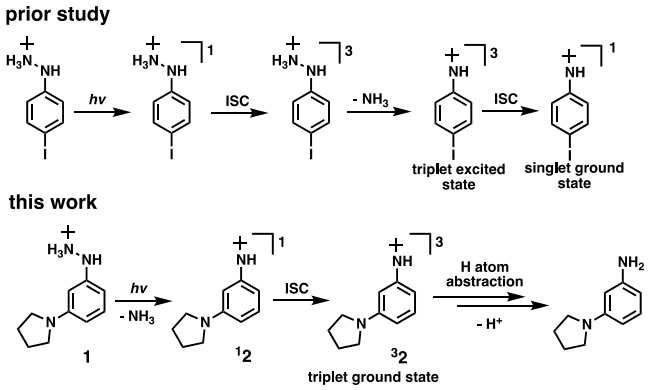

Figure 1. (top) First detection of an excited triplet n, p* state of a nitrenium ion. (bottom) This work provides the first direct detection of a ground state triplet phenyl nitrenium ion.

positions of the benzylic ions with strong π donors (e.g., NH_2) stabilizes an *m*-xylylene-like π, π^* triplet state in preference to the singlet state.[16] This *meta*-effect has recently been validated experimentally, where phenyl oxenium ion exhibits a triplet ground state when appending a π donor on the *meta* position.[19] We anticipated that such an effect should be applicable to phenyl nitrenium ions more broadly.

In this study, we synthesized *m*-pyrrolidinyl-phenyl hydrazine hydrochloride (**1**) as the photoprecursor for the corresponding *m*-pyrrolidinyl-phenyl nitrenium ion (**2**), which includes a robust *meta* π donor (i.e., pyrrolidine). Employing femtosecond (fs-) and nanosecond (ns-) transient absorption (TA) spectroscopy, cryogenic continuous-wave electronic paramagnetic resonance (CW-EPR) spectroscopy, computational analysis, and photoproduct studies, we reveal that nitrenium ion **2** is a π, π^* triplet ground state species with a lifetime of 0.82 μs. Both optical and matrix EPR spectra affirm the discrete existence of the triplet species, and photoproduct studies highlight its radical-like reactivity, which is exemplified by the predominant formation of the stable photoproduct and reduced *m*-pyrrolidinyl-aniline, resulting from sequential H atom abstractions.

EXPERIMENTAL METHODS

Synthesis and Characterization. Detailed synthetic procedures and characterizations of the photoprecursor **1** are given in the Supporting Information. Spectroscopic grade acetonitrile (MeCN) and deionized water were used to prepare the sample solutions for time-resolved spectroscopy experiments. All the mixed solvent ratios are volume ratios unless indicated otherwise.

fs- and ns-TA Spectroscopy. The experimental setups and method for transient absorption experiments have been described in our previous studies.[20,21] The fs-TA experiments were conducted on a commercialized Helios pump−probe system (Ultrafast System) with the femtosecond laser beam from the regenerative amplified Ti:sapphire laser system (Spectra Physics, Spitfire Pro). The laser light (120 fs, 800 nm) was then split into two beams with one used as the pump beam and one as the probe beam. For the present experiments, the wavelength of the pump beam was set as 267 nm (the third harmonic of the fundamental 800 nm), while the probe beam passed through a CaF_2 crystal and generated a white-light continuum (330−650 nm). After the solution was photoexcited by the pump light, the time-delayed probe beam (controlled by the optical delay rail with a maximum temporal delay at 3.3 ns) was passed through the photoexcited solution, and the TA signals were then collected by the detector. A reference probe beam was also used to obtain a better signal-to-noise ratio. The 80 mL sample solutions were prepared with absorbance around 1 at 267 nm and circulated in a 2 mm path-length quartz cuvette. The nanosecond-TA experiments were performed on an LP920 laser flash spectrometer by Edinburgh Instruments Ltd. Briefly, the continuous probe light ranging from 280 to 800 nm was produced by a 450 W ozone free Xe arc lamp, and the 266 nm pump beam was obtained from the fourth harmonic output of an Nd:YAG laser. The 80 mL sample solutions with an absorption of around 1 at 266 nm were prepared in a flowing 1 cm path-length quartz cuvette. The transmitted signals were collected by a photomultiplier detector (for the kinetics mode) and an array detector (for the spectral mode). The instrument response function (irf) of ns-TA is 20 ns.

Continuous-Wave (CW) Electron Paramagnetic Resonance (EPR) Spectroscopy. EPR measurements at the X-band were made on a Bruker ELEXSYS E580 FT-EPR spectrometer incorporated with a temperature control cryostat capable of achieving liquid nitrogen temperatures (80 K) and equipped with a UV-emitting mercury light source channeled into the resonator cavity using a fiber optic cable. **1** is dissolved in anhydrous EtOH at a concentration of 1 mg/mL. The solution is prefrozen to create a glassy matrix to maximize light penetration before being inserted into the resonator. Data collection was performed at various durations of light irradiation. The data were processed and simulated in MATLAB utilizing functions from the EasySpin software package.[22]

Computational Methods. The singlet−triplet gap (ΔE_{ST}) of **2** was estimated using density functional theory (B3LYP/6-31G + (d, p)) and the accurate compound method CBS-QB3. The TD-DFT methodology (TD-B3LYP/6-31G + (d, p)) was performed to predict the UV−vis absorption spectra of the transient species generated from the photolysis of the photoprecursor. The polarizable continuum model (PCM) was also applied when computing the absorption spectra. No imaginary frequency modes were observed in the stationary states of the optimized structures. All of the calculations were performed using the Gaussian 09 program.[23]

Photoproduct Studies. Product studies were conducted using 2.5 mg of precursor **1** dissolved in 1 mL of solvent in a quartz NMR tube. The sample was then subjected to irradiation with 254 nm UV light emitted from a mercury vapor lamp for the desired time intervals in a Rayonet photoreactor. Once the photolysis was complete and confirmed by the disappearance of initial ^{1}H NMR peaks, the sample was submitted to LC-MS using Agilent QTOF 6540 with an ESI ionization method for further product analysis and confirmation.

RESULTS AND DISCUSSION

Theoretical Prediction of the Ground State Electronic Configuration for 2. As shown in Figure 2, the ΔE_{ST} values for **2** were computed to be +5.7 and +7.8 kcal/mol at the level of CBS-QB3 and B3LYP/6-31 + G(d, p) (the restricted method was employed for computing the singlet state). A positive ΔE_{ST} value indicates a triplet ground state. To examine the effects of an unrestricted broken-symmetry approach (UB3LYP) to allow open-shell character in the singlet state, eq 1 was employed to subtract spin contamination from the low-energy triplet state ($\langle S^2 \rangle$ value = 0.63) to yield a spin-purified energy of the singlet state[24]:

$$E_{\text{singlet}} = \frac{2E_{\langle Sz \rangle=0} - \langle S^2 \rangle E_{\langle Sz \rangle=1}}{2 - \langle S^2 \rangle} \quad (1)$$

where E_{singlet} is the corrected singlet energy, $E_{\langle Sz \rangle=0}$ is the broken-symmetry energy, $\langle S^2 \rangle$ is the expectation value of the total-spin operator for the broken-symmetry, and $E_{\langle Sz \rangle=1}$ is the energy of the triplet state at the singlet geometry, as has been done previously. When this broken symmetry approach is taken to allow open-shell character in the singlet state, the singlet−triplet gap lowers by 4.4 kcal/mol in favor of the singlet state (broken-symmetry ΔE_{ST} = +3.4 kcal/mol,

https://doi.org/10.1021/jacs.4c00511
J. Am. Chem. Soc. 2024, 146, 10679−10686

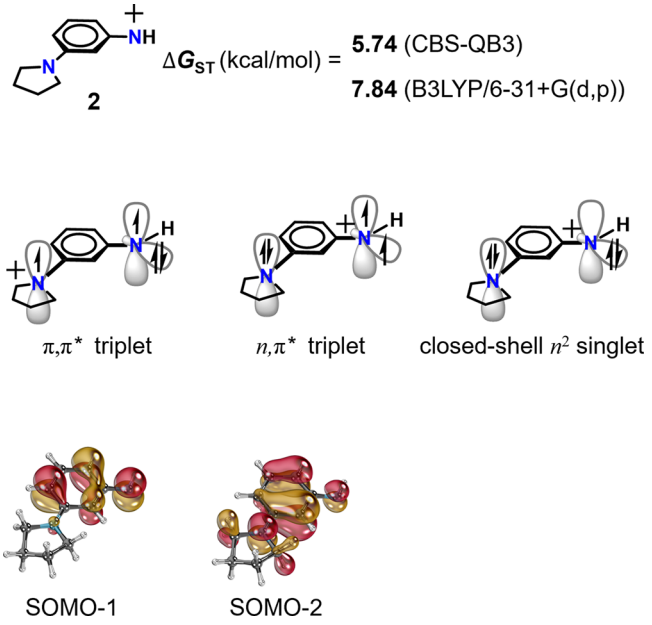

Figure 2. (top) Calculated ΔE_{ST} for **2** using different methods. (middle) Possible schematic electronic configurations for **2**. Computations suggest that the ground state configuration is π,π^* triplet, and the lowest energy singlet state is the closed-shell configuration. (bottom) Visualized Kohn−Sham molecular orbitals for the two SOMO orbitals show the π, π^* nature of the triplet state of ^{3}**2**.

B3LYP/6-31+G(d, p); + 1.3 kcal/mol, CBS-QB3), but the triplet state remains the computed ground state.

These ΔE_{ST} values make a prediction that **2** adopts a triplet ground state. Visualization of the two singly occupied molecular orbitals (SOMOs) in the triplet manifold reveals that the triplet ground state is associated with nondisjoint π, π^* SOMOs, in contrast to the previously observed n, π * triplet state (Figure 1). The nondisjoint SOMOs of **2** leads to large exchange energies favoring the triplet state.[25] Moreover, both SOMOs exhibit delocalized π characters spanning across the phenyl ring and the p orbital of the nitrogen center, indicative of a π, π^* electronic configuration. Figure 2 also illustrates simple schematic models for the lowest electronic states of *meta*-donor-substituted phenyl nitrenium ions. The lowest singlet state is designated "n^2", referring to the occupancy of the HOMO. The lowest triplet state typical of non-*meta* donor aryl nitrenium ions is designated as "n, π^*". This state is derived from the promotion of an electron from the n orbital on the nitrenium center to a π^* orbital, which results from the mixing of the nonbonding orbital on the nitrogen atom and the π^* orbitals of the phenyl ring. Finally, the lowest triplet state of the *meta* π-donors is designated as "π, π^*", indicating that this state is derived from promotion of an electron on a substituent nonbonding orbital of π-symmetry to the π^* level. This can be visualized by starting with the aryl nitrenium ion's singlet state and then transferring an electron from a nonbonding orbital on the donor substituent(s) to the out-of-plane nonbonding orbital on the nitrenium ion center. This would create a species that would have an aminyl radical character at the initial nitrenium ion center and a cation radical site on the *meta* substituent(s). Due to the existence of quinoidal resonance structures for ^{1}**2**, the chemical bonding between the hypovalent nitrogen center and the aryl ring exhibits double bond characteristics, as indicated by the shorter bond length in its singlet state compared to the triplet state of 1.34 Å (triplet) and 1.31 Å (singlet) (see Table S1 in the Supporting Information for all computed bond lengths of the singlet and triplet); this more quinoidal character in the singlet is also observed in the aryl C−C bonds, which feature more bond length alternation in the singlet than the triplet state.

Femtosecond Transient Absorption (fs-TA) Study of 1. Photolysis of **1** was examined using fs-TA experiments performed in 1.4% H_2O in MeCN. The addition of water was employed to aid in the dissolution of the ionic photoprecursors. Once irradiated using a 267 nm pump, within 445 fs, **1** was photoexcited to its higher singlet excited S_n. Following Kasha's rule,[26] it subsequently underwent internal conversion to S_1, whose absorption spectra features a sharp peak at 348 nm and a broad band extending from 390 to 650 nm, centered at 465 nm. Photoheterolysis then occurs spontaneously, as shown in Figure 3a, evidenced by two key observations: (1) a reduction in optical intensity of the initial sharp peak at 348 nm, accompanied by a slight red-shift, and (2) significant narrowing and blue-shifting of the previously broad absorption band, now centered at 430 nm. Over the course of approximately 50 ps, as illustrated in Figure 3b, the spectroscopic characteristics of this singlet state phenyl nitrenium ion are retained, but its optical intensity has a noticeable decay. This process is attributed to vibrational cooling wherein the initially hot-born phenyl nitrenium ion dissipates excess energy to the solvent, a phenomenon that has been observed in the prior work.[19] In the subsequent photochemical process, as displayed in Figure 3c, the prominent peak at 430 nm associated with the singlet phenyl nitrenium ion gradually diminishes in intensity. Concomitantly, a new peak emerges at 355 nm along with the appearance of a broad peak at 506 nm. This process exhibits an isosbestic point at 393 nm, indicating a clean transformation between a precursor species and a product species. This result strongly suggests that the singlet nitrenium ion undergoes a clean transformation, through either a chemical reaction or a change into a distinct electronic configuration.

Global analysis yields four evolution associated difference spectra (EAS) in Figure 3d, corresponding to four distinct kinetic species, whose lifetimes are resolved through time evolution of species population, shown in Figure 3e, as 1.8 ps (black), 19 ps (green), 534 ps (red) and >3 ns (blue). Notably, the decay time constant of the last species (blue) exceeds the time scale of our fs-TA instruments and was further examined using ns-TA, discussed later. The kinetics fit, shown in Figure 3f, exhibits excellent agreement with the experimental data, confirming that the proposed sequential kinetic model effectively represents the experiment data. Assignments of the kinetic species are performed through a comparative analysis, utilizing existing spectroscopic features of singlet nitrenium ions and computed UV−vis spectra that are shown in Figure 3g,h. Though the theoretically predicted UV−vis spectrum of ^{1}**2** exhibits a blue shift, it is important to note that numerous previously reported spectroscopic observations of phenyl nitrenium ions in their singlet state consistently show similar absorption features at approximately 450 nm.[10,27,28] This observed spectroscopic shift, when compared to the computational prediction, can be attributed to the formation of water complexes.[19] Moreover, the homolysis product, aminyl radical, can also be ruled out because of the short lifetime (τ_3 = 534 ps) of this species. Therefore, we assign the species after

https://doi.org/10.1021/jacs.4c00511
J. Am. Chem. Soc. 2024, 146, 10679−10686

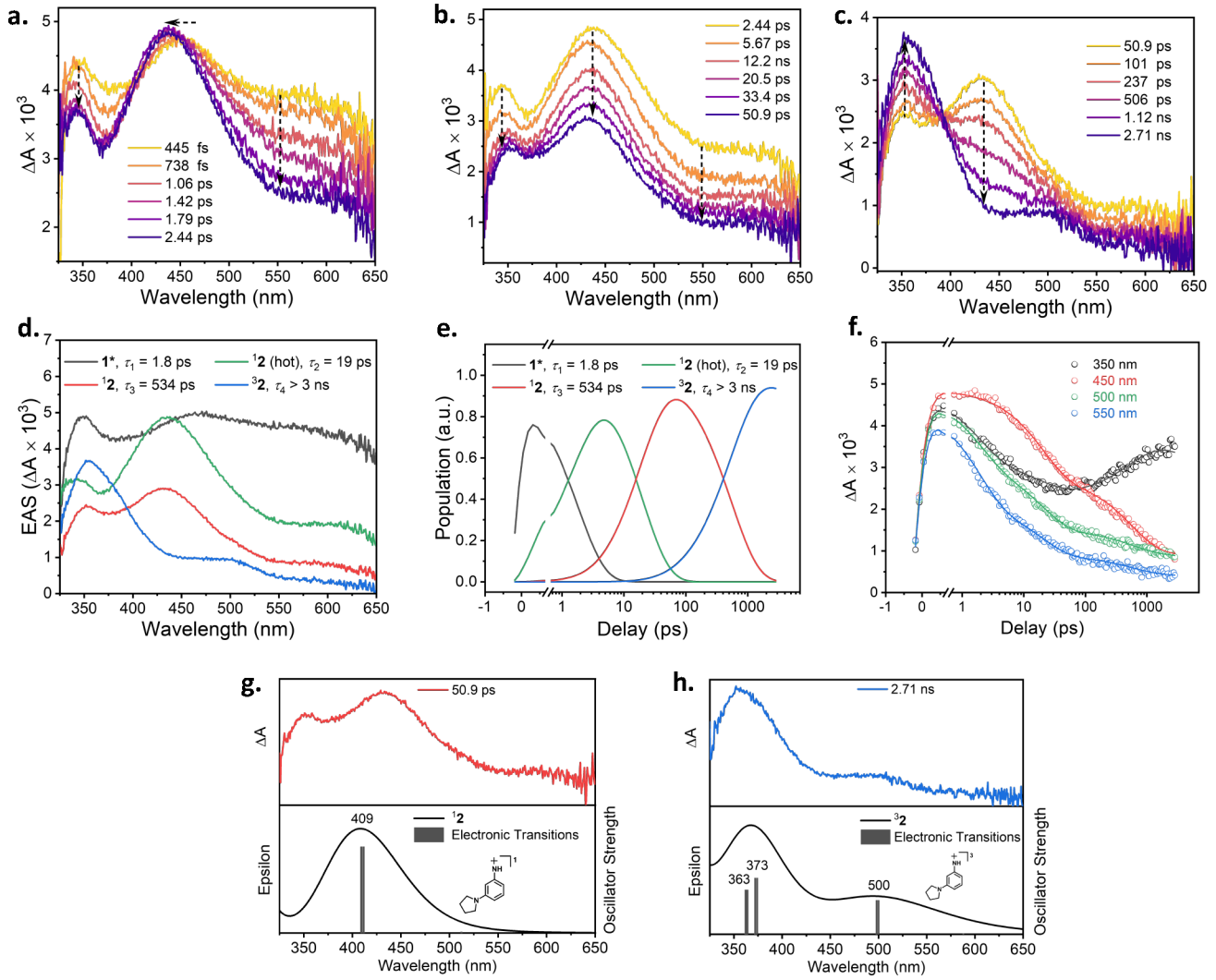

Figure 3. Shown are the fs-TA spectra acquired after 267 nm excitation of the precursor **1** (a) from 445 fs to 2.44 ps, (b) from 2.44 to 50.9 ps, and (c) from 50.9 ps to 2.71 ns. (d) EAS according to the sequential kinetic models. (e) Time evolution of the populations of the kinetic species obtained from the global fitting analysis. Color of the fitting trace is consistent with the EAS spectra. (f) Kinetics fits to the raw data at the indicated wavelengths using the sequential kinetic model. (g) Comparison between (top, red) the experimental data obtained at 50.9 ps and (bottom) the calculated UV−vis spectra of ^{1}**2** (closed-shell n^2 singlet). (h) Comparison between (top, blue) the experimental data obtained at 2.71 ns and (bottom) the calculated UV−vis spectra of ^{3}**2** (π, π^* triplet).

the photoexcited photo precursor to ^{1}**2** formed from an excited state photoheterolysis process.

It is noteworthy that the lifetime of this singlet nitrenium ion is still considerably shorter than most detected phenyl nitrenium ions, which typically have lifetimes exceeding hundreds of nanoseconds to microseconds by reacting with surrounding nucleophiles due to its electron-deficient nature and associated resonant structures (Scheme S2, Supporting Information).[1,2] A difference is that with this nitrenium ion the ground state of this phenyl nitrenium ion is calculated to be the triplet state. Although the nitrenium ion is initially generated in a singlet spin state due to the spin-conserving nature of the photoheterolysis step, it relaxes to its ground state, a π, π^* triplet though ISC. The relatively small computed singlet−triplet energy gap further facilitates this transition from the singlet state to the triplet spin multiplicity. Consequently, we attribute the transformation depicted in Figure 3c to the ISC process. Additionally, the computed UV−vis spectrum presented in Figure 3g for ^{3}**2** aligns well with the experimental spectrum extracted at 2.7 ns.

Nanosecond Transient Absorption (ns-TA) Study of 1. To provide the integrated spectra of the latter species beyond 3 ns, ns-TA was employed to study the reaction pathways of precursor **1** in 1.4% H_2O in MeCN after irradiation. Figure 4a shows that the absorption band at 355 nm, associated with ^{3}**2**, continues to increase in intensity and slightly red-shifts to 375 nm. Simultaneously, the broad band centered at 506 nm undergoes a significant red shift to 550 nm, accompanied by a broader feature. These changes unambiguously demonstrate a new transient species has formed. The temporal dependences of the transient absorption intensity at 375 nm can be mathematically fitted by a monoexponential function, as displayed in Figure 4b, which gives a time constant of τ_4 = 0.82 μs, representing the lifetime of ^{3}**2** that complements the fs-TA analysis. Importantly, the optical spectrum of the generated species closely matches the computed UV−vis spectrum of the *m*-pyrrolidinyl-phenyl aminyl radical (**3**). This radical species is expected to derive from ^{3}**2** through a process involving H atom abstraction and subsequent deprotonation. Such radical reactivity of ^{3}**2** is

https://doi.org/10.1021/jacs.4c00511
J. Am. Chem. Soc. 2024, 146, 10679−10686

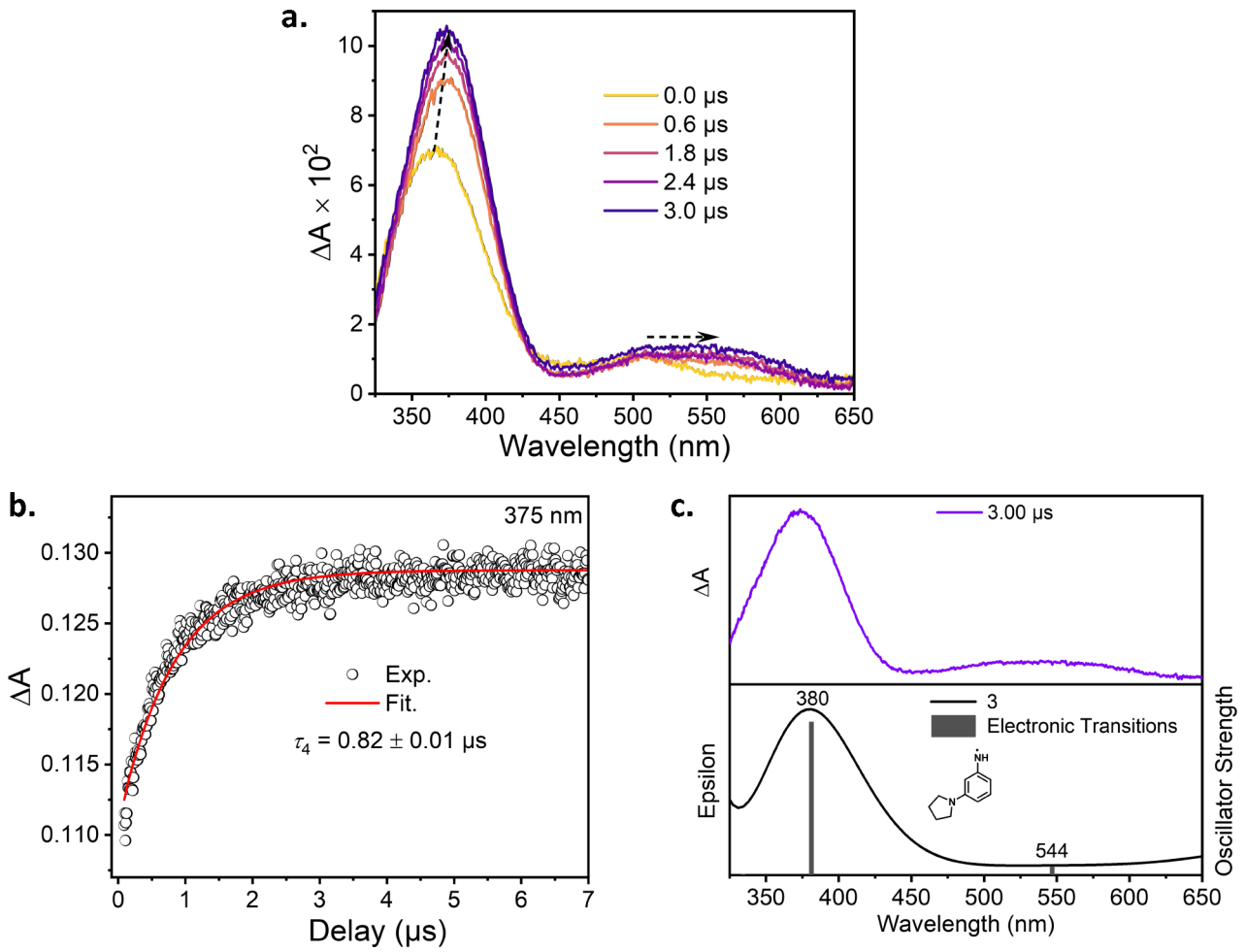

Figure 4. (a) Shown are ns-TA spectra acquired from 0 μs (irf = 20 ns) to 440 μs. (b) Temporal dependences of the transient absorption intensity of initial compound at 375 nm in the long time region. Solid red line indicates fittings using a monoexponential function. (c) Comparison of (top, purple) the experimental data obtained at 3.00 μs and (bottom) the calculated UV−vis spectra of **3** (aminyl radical).

anticipated as the triplet state can be conceptually interpreted as comprising two radical centers with a certain degree of exchange or dipolar coupling. The assignment of **3** is further corroborated in the photoproduct studies discussed later in the context, where the primary photoproduct is the reduced *m*-pyrrolidinyl-aniline. **3** has a long lifetime of τ_5 = 487 μs in solutions before it produces the ultimate photoproduct. (Figure S8, Supporting Information).

Cryogenic CW-EPR Study of 1. Additional evidence supporting the ground state of **2** as a triplet state comes from low-temperature matrix isolation EPR experiments. At cryogenic temperatures, most nontunneling reactions are effectively suppressed due to the lack of activation energy. Moreover, the frozen matrix constrains molecular motions, preventing chemical reactions. Furthermore, operating at 80 K, which corresponds to a thermal energy (RT) of only 0.16 kcal/mol, essentially no thermal population of an excited triplet state would be possible, although a species with effectively degenerate singlet−triplet energies cannot be ruled out. To probe the triplet signal of ^{3}**2**, a photolysis study of **1** within a low-temperature EtOH glassy matrix at 80 K was conducted. As shown in Figure 5a, continuous light irradiation leads to the progressive growth of a paramagnetic species, indicating ongoing photolysis. The resulting species are effectively locked within the rigid solid environment, enabling an exploration of their spin states. The broad signal, which exceeds 20 mT in the EPR spectra, strongly suggests the formation of a triplet diradical species rather than an S = 1/2 species. However, a monoradical impurity is also present, possibly arising from a competitive homolysis pathway in the solid state or H atom transfer from nearby the pyrrolidinyl group. The convoluted spectra can be simulated by as a sum of contributions from both a triplet species and a monoradical impurity (Figure S7, Supporting Information) to obtain the zero-field splitting (ZFS) parameters: the $|D|/hc$ parameter (0.0048 cm^{-1}), $|E|/hc$ parameter (0.0002 cm^{-1}), and $E/|D|$ = 0.045 G = 1.5 × 10^{-6} cm^{-1}. In general, the $|D|/hc$ tensor of non-Kekule diradicals are about an order of magnitude smaller compared to atom-centered nitrenes[29,30] or carbenes,[31] and those in ^{3}**2** are smaller than the analogous triplet meta-xylylene-like diradical species[32,33] possessing similar electronic architectures, suggesting a larger spin distance. In the dipolar model, $|D|/hc$ = 1.299 g·cm^{-1} Å$^3/r^3$, where r is the distance between interacting electrons in angstroms and g is the electron g-value.[34−36] This dipolar approximation suggests a spin distance of ∼8 Å for ^{3}**2** from the $|D|/hc$ value, while the computed distance between the nitrenium nitrogen and the pyrrolidinyl nitrogen, the presumed spin sites, is ∼5 Å. Delocalization of one of the spins onto the alkyl chains of the pyrrolidinyl ring (Figure 2), as shown in one of the SOMOs, may lead to a longer spin

https://doi.org/10.1021/jacs.4c00511
J. Am. Chem. Soc. 2024, 146, 10679−10686

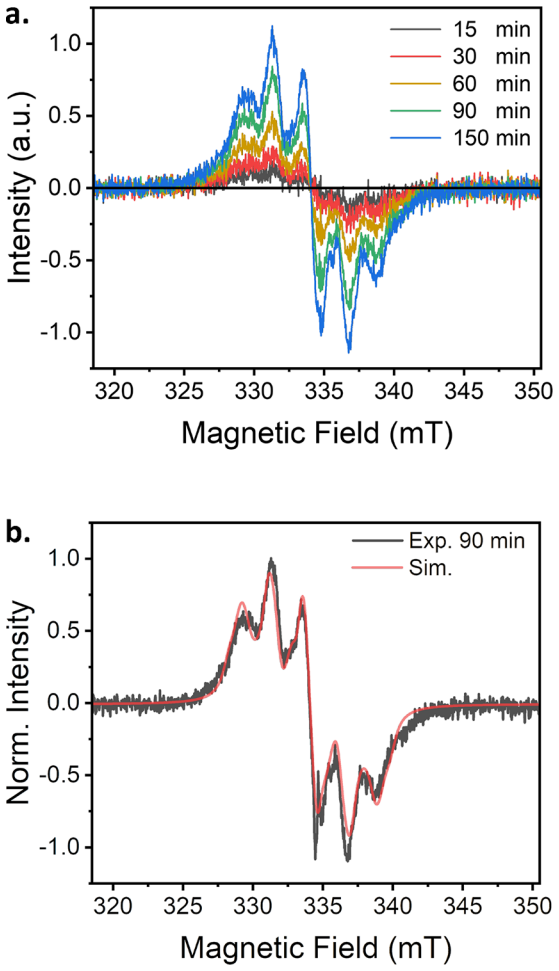

Figure 5. (a) EPR spectra recorded under different durations of UV light irradiation. (b) Experimental EPR data collected after 90 min of irradiation (black), overlaid with the simulation (red). D = 144 G; $|D|/hc$ = 0.0048 cm^{-1}; E = 6.5 G; $|E|/hc = 2.0 \times 10^{-4}$ cm^{-1}. Detailed simulation parameters can be found in the Supporting Information.

distance. Notably, the absence of the forbidden double quantum $\Delta m_s = 2$ transition aligns with this small $|D|$ value. Considering the small ZFS values, the Zeeman splitting for the forbidden transition (half-field transition) $\Delta m_s = 2$ on the X band (~9.8 GHz) is anticipated to be very small. As a result, the signal corresponding to the microwave-resonant transition is either quickly relaxed or the signal-to-noise ratio is too low to be observed.

Photoproduct Study of 1 and Proposed Photolysis Pathway. The proposed mechanism fitting the data is shown in Scheme 1. Photolysis generates initially a singlet nitrenium that undergoes ISC to generate the triplet ground state nitrenium ion. A triplet ground state of **2** is further supported by the photoproduct analysis, which was performed in 1.4% H_2O in MeCN or in H_2O. ^1H NMR characterization was used to determine the completion of the photolysis, and LC-MS was used to isolate photoproducts for further analysis and product confirmation. Figures S4–S6 in the Supporting Information show that the predominant product is the reduced *m*-pyrrolidinyl-aniline, suggesting the radical-like reactivity of the triplet nitrenium ion ^{3}**2**. Additionally, some nucleophilic adducts with water and chloride are observed, likely originating from reactions of initially generated ^{1}**2** with the Cl counterion in the precursor or with water. Competing against the ISC

Scheme 1. Proposed Mechanistic Pathway

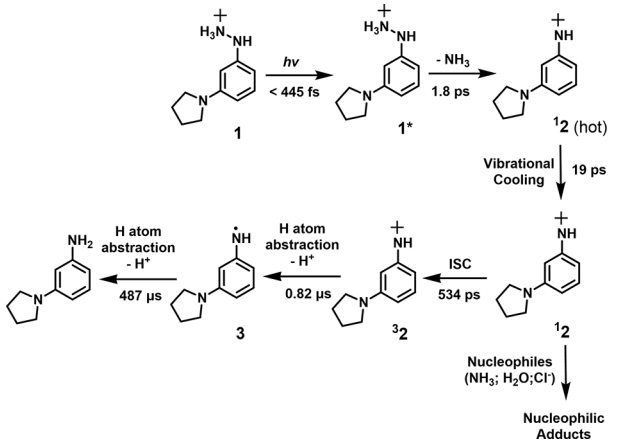

conversion within 534 ps, nucleophilic addition acts as a concomitant singlet decay channel. As mentioned earlier, nucleophile adducts of a singlet phenyl nitrenium ion are typically expected due to the presence of resonance structures that create carbon cations on the phenyl aromatic ring (Scheme S2, Supporting Information).

The reactivity of triplet phenyl nitrenium ions has received limited attention due to their infrequent occurrence, but by drawing parallels with related reactive intermediates, such as carbenes and nitrenes, one might anticipate radical ion chemistry, including processes like H atom abstraction or electron transfer. The formation of the reduced product resulting from the photolysis of **1** suggests a triplet nitrenium ion reacting through sequential H atom abstraction processes, possibly from MeCN solvent or from unreacted **1**, followed by proton loss rather than nucleophilic trapping chemistry. Moreover, the H atom abstraction reactions that happen at the cationic radical and aminyl radical centers of ^{3}**2** have been extensively documented in the literature.[37−39]

CONCLUSIONS

In conclusion, a new photoprecursor for the generation of the phenyl nitrenium ion, *m*-pyrrolidinyl-phenyl nitrenium ion (**2**), was investigated using time-resolved optical spectroscopic experiments (fs-TA, and ns-TA) and EPR measurements along with computational calculations and photochemical product studies. These experiments allow us to draw several conclusions. First, **2** has a π, π^* triplet ground state, in contrast to the excited n, π^* triplet phenyl nitrenium ion reported previously.[14] Its reactivity engages in H atom abstractions to yield a reduced product, which is rather similar to triplet carbenes. Furthermore, this π, π^* triplet ground state of this nitrenium ion is 0.8 μs, which is longer-lived than typical closed-shell phenyl nitrenium ions and similar to the diminished reactivity of triplet carbenes compared to singlet carbenes. Future work will focus on the intriguing possibilities of using this photochemically generated triplet nitrenium ion for practical synthetic and organomagnetic applications.

ASSOCIATED CONTENT

Supporting Information

The Supporting Information is available free of charge at https://pubs.acs.org/doi/10.1021/jacs.4c00511.

Spectral data (^1H NMR, ^{13}C NMR, HRMS) for the newly synthesized compounds, computational coordi-

https://doi.org/10.1021/jacs.4c00511
J. Am. Chem. Soc. 2024, 146, 10679−10686

nates, and absolute energies, photolysis product studies, additional TA spectra, and EPR simulations (PDF)

AUTHOR INFORMATION

Corresponding Authors

David Lee Phillips − *Department of Chemistry, University of Hong Kong, Hong Kong 11111, P. R. China;* orcid.org/0000-0002-8606-8780; Email: phillips@hku.hk

Arthur H. Winter − *Department of Chemistry, Iowa State University, Ames, Iowa 50011, United States;* orcid.org/0000-0003-2421-5578; Email: winter@iastate.edu

Authors

Yunfan Qiu − *Department of Chemistry, Iowa State University, Ames, Iowa 50011, United States;* orcid.org/0000-0002-4666-1424

Lili Du − *Department of Chemistry, University of Hong Kong, Hong Kong 11111, P. R. China;* orcid.org/0000-0002-9712-3925

Sarah D. Cady − *Department of Chemistry, Iowa State University, Ames, Iowa 50011, United States*

Complete contact information is available at: https://pubs.acs.org/10.1021/jacs.4c00511

Funding

NSF CHE-2055335 PRF 62317-ND4

Notes

The authors declare no competing financial interest.

ACKNOWLEDGMENTS

A.H.W. thanks PRF 62317-ND4 and the National Science Foundation for supporting this work through CHE-2055335. D.L.P. thanks support from the Hong Kong Research Grants Council (GRF 17302419, GRF 17316922), The University of Hong Kong Development Fund 2013-2014 project "New Ultrafast Spectroscopy Experiments for Shared Facilities", Major Program of Guangdong Basic and Applied Research (2019B030302009), Key-Area Research and Development Program of Guangdong Province (2020B0101370003), and URC Seed Funding for Strategic Interdisciplinary Research Scheme (SIRS) 2019/20.

REFERENCES

(1) Moss, R. A.; Platz, M.; Jones, M., Jr. *Reactive Intermediate Chemistry*; Wiley, 2004.

(2) Falvey, D. E.; Gudmundsdottir, A. D. *Nitrene and Nitrenium Ions*; Wiley, 2013.

(3) Radomski, J. L.; Brill, E. Bladder Cancer Induction by Aromatic Amines: Role of N-Hydroxy Metabolites. *Science* **1970**, *167* (3920), 992−993.

(4) Knize, M. G.; Cunningham, P. L.; Griffin, E. A.; Jones, A. L.; Felton, J. S. Characterization of Mutagenic Activity in Cooked-Grain-Food Products. *Food Chem. Toxicol.* **1994**, *32* (1), 15−21.

(5) Lux, F. Properties of electronically conductive polyaniline: a comparison between well-known literature data and some recent experimental findings. *Polymer* **1994**, *35* (14), 2915−2936.

(6) Novak, M.; Kahley, M. J.; Eiger, E.; Helmick, J. S.; Peters, H. E. Reactivity and Selectivity of Nitrenium Ions Derived from Ester Derivatives of Carcinogenic N-(4-Biphenylyl)hydroxylamine and the Corresponding Hydroxamic Acid. *J. Am. Chem. Soc.* **1993**, *115* (21), 9453−9460.

(7) Suzuki, H.; Ninoseki, T.; Hayashi, A.; Hase, Y.; Matsui, T.; Naito, M.; Sugai, S. Comparison of Stabilities of Nitrenium Ions and in vitro and in vivo Genotoxic Potential, between Four Aniline Derivatives. *Fundam. Toxicol. Sci.* **2018**, *5* (1), 21−32.

(8) Turesky, R. J.; Le Marchand, L. Metabolism and Biomarkers of Heterocyclic Aromatic Amines in Molecular Epidemiology Studies: Lessons Learned from Aromatic Amines. *Chem. Res. Toxicol.* **2011**, *24* (8), 1169−1214.

(9) Skipper, P. L.; Kim, M. Y.; Sun, H. L. P.; Wogan, G. N.; Tannenbaum, S. R. Monocyclic Aromatic Amines as Potential Human Carcinogens: Old is New Again. *Carcinogenesis* **2010**, *31* (1), 50−58.

(10) McClelland, R. A.; Ahmad, A.; Dicks, A. P.; Licence, V. E. Spectroscopic Characterization of the Initial C8 Intermediate in the Reaction of the 2-Fluorenylnitrenium Ion with 2'-Deoxyguanosine. *J. Am. Chem. Soc.* **1999**, *121* (14), 3303−3310.

(11) Cramer, C. J.; Dulles, F. J.; Falvey, D. E. Ab Initio Characterization of Phenylnitrenium and Phenylcarbene: Remarkably Different Properties for Isoelectronic Species. *J. Am. Chem. Soc.* **1994**, *116* (21), 9787−9788.

(12) Anderson, G. B.; Yang, L. L. N.; Falvey, D. E. Photogenerated Arylnitrenium Ions: Photoisomerization of the N-tert-Butyl-3-methylanthranilium Ion and Spin-Selective Reactivity of the Isomeric Arylnitrenium Ion. *J. Am. Chem. Soc.* **1993**, *115* (16), 7254−7262.

(13) Srivastava, S.; Falvey, D. E. Reactions of a Triplet Arylnitrenium Ion: Laser Flash Photolysis and Product Studies of N-tert-Butyl(2-acetyl-4-nitrophenyl)nitrenium Ion. *J. Am. Chem. Soc.* **1995**, *117* (41), 10186−10193.

(14) Du, L.; Wang, J.; Qiu, Y.; Liang, R.; Lu, P.; Chen, X.; Phillips, D. L.; Winter, A. H. Generation and Direct Observation of a Triplet Arylnitrenium Ion. *Nat. Commun.* **2022**, *13* (1), 3458 DOI: 10.1038/s41467-022-31091-z.

(15) Qiu, Y.; Winter, A. H. Anomalous Electronic Properties of Iodous Materials: Application to High-Spin Reactive Intermediates and Conjugated Polymers. *J. Org. Chem.* **2020**, *85* (6), 4145−4152.

(16) Winter, A. H.; Falvey, D. E.; Cramer, C. J. Effect of meta Electron-Donating Groups on the Electronic Structure of Substituted Phenyl Nitrenium Ions. *J. Am. Chem. Soc.* **2004**, *126* (31), 9661−9668.

(17) Qiu, Y.; Fischer, L. J.; Dutton, A. S.; Winter, A. H. Aryl Nitrenium and Oxenium Ions with Unusual High-Spin π,π^* Ground States: Exploiting (Anti)Aromaticity. *J. Org. Chem.* **2017**, *82* (24), 13550−13556.

(18) Sullivan, M. B.; Brown, K.; Cramer, C. J.; Truhlar, D. G. Quantum Chemical Analysis of para-Substitution Effects on the Electronic Structure of Phenylnitrenium Ions in the Gas Phase and Aqueous Solution. *J. Am. Chem. Soc.* **1998**, *120* (45), 11778−11783.

(19) Li, M.-D.; Albright, T. R.; Hanway, P. J.; Liu, M.; Lan, X.; Li, S.; Peterson, J.; Winter, A. H.; Phillips, D. L. Direct Spectroscopic Detection and EPR Investigation of a Ground State Triplet Phenyl Oxenium Ion. *J. Am. Chem. Soc.* **2015**, *137* (32), 10391−10398.

(20) Du, L.; Li, M.-D.; Zhang, Y.; Xue, J.; Zhang, X.; Zhu, R.; Cheng, S. C.; Li, X.; Phillips, D. L. Photoconversion of β-Lapachone to α-Lapachone via a Protonation-Assisted Singlet Excited State Pathway in Aqueous Solution: A Time-Resolved Spectroscopic Study. *J. Org. Chem.* **2015**, *80* (15), 7340−7350.

(21) Li, M.-D.; Ma, J.; Su, T.; Liu, M.; Yu, L.; Phillips, D. L. Direct Observation of Triplet State Mediated Decarboxylation of the Neutral and Anion Forms of Ketoprofen in Water-Rich, Acidic, and PBS Solutions. *J. Phys. Chem. B* **2012**, *116* (20), 5882−5887.

(22) Stoll, S.; Schweiger, A. EasySpin, a Comprehensive Software Package for Spectral Simulation and Analysis in EPR. *J. Magn. Reson.* **2006**, *178* (1), 42−55.

(23) Frisch, M. J.; Ti, G. W.; Schlegel, H. B.; Scuseria, G. E.; Robb, M. A.; Cheeseman, J. R.; Scalmani, G.; Barone, V.; Petersson, G. A.; Nakatsuji, H.; Li, X.; Caricato, M.; Marenich, A.; Bloino, J.; Janesko, B. G.; Gomperts, R.; Mennucci, B.; Hratchian, H. P.; Ortiz, J. V.; Izmaylov, A. F.; Sonnenberg, J. L.; Williams-Young, D.; Ding, F.; Lipparini, F.; Egidi, F.; Goings, J.; Peng, B.; Petrone, A.; Henderson, T.; Ranasinghe, D.; Zakrzewski, V. G.; Gao, J.; Rega, N.; Zheng, G.; Liang, W.; Hada, M.; Ehara, M.; Toyota, K.; Fukuda, R.; Hasegawa, J.; Ishida, M.; Nakajima, T.; Honda, Y.; Kitao, O.; Nakai, H.; Vreven, T.;

Throssell, K.; Montgomery, J. A., Jr.; Peralta, J. E.; Ogliaro, F.; Bearpark, M.; Heyd, J. J.; Brothers, E.; Kudin, K. N.; Staroverov, V. N.; Keith, T.; Kobayashi, R.; Normand, J.; Raghavachari, K.; Rendell, A.; Burant, J. C.; Iyengar, S. S.; Tomasi, J.; Cossi, M.; Millam, J. M.; Klene, M.; Adamo, C.; Cammi, R.; Ochterski, J. W.; Martin, R. L.; Morokuma, K.; Farkas, O.; Foresman, J. B.; Fox, D. J., Gaussian, Inc.: Wallingford CT, 2016.

(24) Yamaguchi, K.; Jensen, F.; Dorigo, A.; Houk, K. N. A Spin Correction Procedure for Unrestricted Hartree-Fock and Møller-Plesset Wavefunctions for Singlet Diradicals and Polyradicals. *Chem. Phys. Lett.* **1988**, *149* (5−6), 537−542.

(25) Borden, W. T.; Iwamura, H.; Berson, J. A. Violations of Hund's Rule in Non-Kekule Hydrocarbons: Theoretical Prediction and Experimental Verification. *Acc. Chem. Res.* **1994**, *27* (4), 109−116.

(26) Kasha, M. Characterization of Electronic Transitions in Complex Molecules. *Disc. Faraday Soc.* **1950**, *9*. 14.

(27) Srivastava, S.; Ruane, P. H.; Toscano, J. P.; Sullivan, M. B.; Cramer, C. J.; Chiapperino, D.; Reed, E. C.; Falvey, D. E. Structures of Reactive Nitrenium Ions: Time-Resolved Infrared Laser Flash Photolysis and Computational Studies of Substituted N-Methyl-N-arylnitrenium Ions. *J. Am. Chem. Soc.* **2000**, *122* (34), 8271−8278.

(28) Davidse, P. A.; Kahley, M. J.; McClelland, R. A.; Novak, M. Flash Photolysis Observation and Lifetimes of 2-Fluorenyl- and 4-Biphenylylacetylnitrenium Ions in Aqueous Solution. *J. Am. Chem. Soc.* **1994**, *116* (10), 4513−4514.

(29) Kvaskoff, D.; Bednarek, P.; George, L.; Waich, K.; Wentrup, C. Nitrenes, Diradicals, and Ylides. Ring Expansion and Ring Opening in 2-Quinazolylnitrenes. *J. Org. Chem.* **2006**, *71* (11), 4049−4058.

(30) Chapyshev, S. V.; Korchagin, D. V.; Budyka, M. F.; Gavrishova, T. N.; Neuhaus, P.; Sander, W. EPR Studies on Branched High-Spin Arylnitrenes. *ChemPhysChem* **2012**, *13* (11), 2721−2728.

(31) Costa, P.; Sander, W. Hydrogen Bonding Switches the Spin State of Diphenylcarbene from Triplet to Singlet. *Angew. Chem., Int. Ed.* **2014**, *53* (20), 5122−5125.

(32) Wright, B. B.; Platz, M. S. Electron Spin Resonance Spectroscopy of the Triplet State of m-Xylylene. *J. Am. Chem. Soc.* **1983**, *105* (3), 628−630.

(33) Olankitwanit, A.; Pink, M.; Rajca, S.; Rajca, A. Synthesis of Aza-m-Xylylene Diradicals with Large Singlet−Triplet Energy Gap and Statistical Analyses of Their EPR Spectra. *J. Am. Chem. Soc.* **2014**, *136* (40), 14277−14288.

(34) Minato, M.; Lahti, P. M. Zero-Field Splitting versus Interelectronic Distance in Triplet Electron Spin Resonance Spectra of Localized Dinitrenes. *J. Phys. Org. Chem.* **1993**, *6* (8), 483−487.

(35) Adam, W.; Kita, F.; Harrer, H. M.; Nau, W. M.; Zipf, R. The D Parameter (EPR Zero-Field Splitting) of Localized 1,3-Cyclopentanediyl Triplet Diradicals as a Measure of Electronic Substituent Effects on the Spin Densities in Para-Substituted Benzyl-Type Radicals. *J. Org. Chem.* **1996**, *61* (20), 7056−7065.

(36) Eaton, S. S.; More, K. M.; Sawant, B. M.; Eaton, G. R. Use of the ESR Half-Field Transition to Determine the Interspin Distance and the Orientation of the Interspin Vector in Systems with Two Unpaired Electrons. *J. Am. Chem. Soc.* **1983**, *105* (22), 6560−6567.

(37) Ganley, J. M.; Murray, P. R. D.; Knowles, R. R. Photocatalytic Generation of Aminium Radical Cations for C−N Bond Formation. *ACS Catal.* **2020**, *10* (20), 11712−11738.

(38) Su, Z.; Mariano, P. S.; Falvey, D. E.; Yoon, U. C.; Oh, S. W. Dynamics of Anilinium Radical α-Heterolytic Fragmentation Processes. Electrofugal Group, Substituent, and Medium Effects on Desilylation, Decarboxylation, and Retro-Aldol Cleavage Pathways. *J. Am. Chem. Soc.* **1998**, *120* (41), 10676−10686.

(39) Pratley, C.; Fenner, S.; Murphy, J. A. Nitrogen-Centered Radicals in Functionalization of sp2 Systems: Generation, Reactivity, and Applications in Synthesis. *Chem. Rev.* **2022**, *122* (9), 8181−8260.

https://doi.org/10.1021/jacs.4c00511
J. Am. Chem. Soc. 2024, 146, 10679−10686